UC San Diego

UC San Diego Previously Published Works

Title

BathyBoard: A Surfboard-Based Platform for Measuring Surf Zone Bathymetry

Permalink

https://escholarship.org/uc/item/6x72q9vh

Journal

Journal of Surveying Engineering, 153(1)

ISSN

0733-9453 1943-5428

Authors

Pick, Kanoa

Quinn, Kaden

Cirrito, Nicholas

et al.

Publication Date

2027-11-14

DOI

10.1061/JSUED2.SUENG-1758

Peer reviewed

eScholarship.org Powered by the California Digital Library
University of California

BathyBoard: A Surfboard-Based Platform for Measuring Surf Zone Bathymetry

Kanoa Pick[1], Kaden Quinn[2,3], Nicholas Cirrito[4], Ashton Domi[5], Georgios Tsampras[6], and Falk Feddersen[7]

[1]PhD Student, Scripps Institution of Oceanography, University of California San Diego, La Jolla, CA 92093-0209, USA (corresponding author). Email: kpick@ucsd.edu.

[2]Oak Ridge Institute for Science and Education Fellow, USACE Engineer Research and Development Center Field Research Facility, 1261 Duck Rd., Kitty Hawk, NC 29797, USA

[3]Visiting Scholar, Scripps Institution of Oceanography, University of California San Diego, La Jolla, CA 92093-0209, USA

[4]PhD Student, Scripps Institution of Oceanography, University of California San Diego, La Jolla, CA 92093-0209, USA

[5]PhD Student, Scripps Institution of Oceanography, University of California San Diego, La Jolla, CA 92093-0209, USA

[6]Associate Professor, Department of Structural Engineering, University of California San Diego, La Jolla, CA 92093-0448, USA

[7]Professor, Scripps Institution of Oceanography, University of California San Diego, La Jolla, CA 92093-0209, USA

ABSTRACT

Bathymetric data in surf zone environments are vital for coastal monitoring and hazard assessment, yet these regions remain challenging to survey due to shallow water and breaking waves. Jet ski based survey methods are highly effective for rapidly mapping large stretches of coastline, but their cost, transport difficulties, permitting requirements, and safety limitations can restrict deployment, particularly in shallow water areas with swimmers and surfers. This study presents the *BathyBoard*, a low-cost bathymetric survey platform designed to address this observational gap. The platform is portable, can be transported on commercial aircraft to remote locations, operates safely around swimmers and surfers, and can collect data near breaking waves in targeted areas. The system integrates an echo sounder and a Global Navigation Satellite System (GNSS) receiver on a surfboard-based platform. A GNSS-based wave correction methodology was

used to remove wave-induced free-surface fluctuations from echo sounder measurements. Spectral analysis demonstrated strong agreement between GNSS elevation fluctuations and echo sounder depth fluctuations within the sea-swell frequency band, indicating that both sensors respond to the same wave motions. The performance of the *BathyBoard* was evaluated against two bathymetric datasets. Comparisons with a sonar-equipped survey jet ski along cross-shore transects near Scripps Pier, California, showed excellent agreement between the two platforms, while demonstrating the ability of the *BathyBoard* to collect measurements in appreciably shallower water. Repeated cross-shore transects demonstrated consistent bathymetric measurements. Additional validation was performed at two coral reef sites on the south shore of O‘ahu, Hawai‘i, against topobathymetric aerial Light Detection And Ranging (LiDAR) data. Strong agreement was observed between *BathyBoard* and LiDAR bathymetry at both sites. These results demonstrate that the *BathyBoard* provides an effective, low-cost approach for expanding access to high-resolution bathymetric surveys in shallow, historically data-deficient coastal environments.

PRACTICAL APPLICATIONS

Shallow coastal waters and surf zones are among the most difficult places to collect bathymetric (seafloor depth) measurements, yet accurate bathymetry is essential for understanding wave breaking, coastal flooding, and erosion processes. Vessel-based platforms, including boats and jet skis, are costly and can be limited by shallow water and breaking waves, whereas similarly expensive remote-sensing methods depend on water clarity and environmental conditions. This study introduces the *BathyBoard*, a low-cost, human-powered survey platform that combines a sonar depth sensor and Global Navigation Satellite System (GNSS) receiver to measure bathymetry while being paddled by a single operator. The platform can survey targeted surf zone areas that may be unsuitable for other vessels, provided site and wave conditions permit safe operation by a proficient operator. *BathyBoard* observations agreed strongly with a sonar-equipped jet ski survey system on a sandy California beach and airborne Light Detection And Ranging (LiDAR) measurements of coral reefs in Hawai‘i. It therefore complements existing survey methods by providing a portable and economical option for high-resolution measurements in surf zones that have historically been difficult and expensive to survey.

INTRODUCTION

Mapping the nearshore bathymetry of coral reefs, rocky coastlines, and sandy beaches is fundamental to understanding coastal processes and managing shoreline change. Knowledge of coral reef bathymetry

is necessary to decipher how reef morphology influences wave transformation, breaking, and dissipation (e.g., Lowe et al., 2005). Reef and channel geometry strongly affect wave setup and circulation patterns (e.g., Lowe et al., 2009), with important implications for coastal flooding and ecosystem health. Accurate bathymetry along rocky shorelines is also important for parameterizing bottom friction in wave models (e.g., Marques et al., 2025). High-resolution bathymetric observations of sandy beaches are used to quantify sediment budgets (e.g., Ludka et al., 2018; Seymour et al., 2005), track sandbar evolution (e.g., Gallagher et al., 1998), and inform coastal protection strategies. These measurements contribute to long-term beach profile records (e.g., Ludka et al., 2019; Turner et al., 2016) and are used to evaluate equilibrium shoreline response models (e.g., Ludka et al., 2015; Yates et al., 2009). Nearshore bathymetry also provides the bottom boundary for coastal hydrodynamic and morphodynamic models (e.g., Bak et al., 2019; Luijendijk et al., 2017). Despite its importance, the evolution of sandy beach bathymetry remains difficult to observe and predict. Morphologic changes can occur on hourly to daily timescales (Brodie et al., 2018; Gallagher et al., 1998), yet the processes governing this variability are not fully understood and are often poorly captured by existing models. A key limitation is the difficulty of obtaining frequent, high-quality measurements in the surf zone, where depth-limited breaking waves, strong currents, and interactions with beachgoers create hazardous conditions for traditional survey methods.

Remote sensing enables large area bathymetric mapping without exposing surveyors to hazards in the surf zone. Satellite-derived bathymetry provides broad spatial coverage and can be repeatedly collected over regional to global scales. In optically clear waters, depth can be estimated from multispectral imagery by relating depth-dependent attenuation of visible light to variations in ocean color (e.g., Frugier et al., 2026). Satellite video has also enabled the extraction of wave kinematics, where the propagation of wave crests is tracked through time and inverted for water depth (e.g., O'Dea et al., 2025). However, satellite-derived bathymetry remains limited by image resolution, water clarity, and cloud cover. Unmanned aerial vehicle (UAV) based methods via cameras or Light Detection And Ranging (LiDAR), combined with bathymetry inversion techniques (e.g., Holman et al., 2013) can resolve nearshore bathymetry at higher spatial and temporal resolutions over shorter time-scales (e.g., Brodie et al., 2019; Lange et al., 2023). X-band radar systems have also been used to estimate bathymetry from sea-surface roughness (e.g., Honegger et al., 2019). The sea state requirements of these remote sensing approaches differ. Multispectral and LiDAR methods generally benefit from calm, clear water, whereas wave kinematic and X-band radar methods require sufficient surface wave activity to extract bathymetry.

Portable uncrewed surface vehicles have been developed to enable bathymetric surveying within the surf zone (e.g., Francis and Traykovski, 2021). Uncrewed crawler vehicles have also been deployed for surf zone bathymetric surveys (e.g., Bak et al., 2023). Both uncrewed surface and crawler vehicles support autonomous waypoint navigation and shore-based supervision, keeping personnel safely out of the surf zone during data collection. However, such systems are costly and not feasible for low-budget operations. Larger seabed-contact survey vehicles, such as the Coastal Research Amphibious Buggy (CRAB) (e.g., Birkemeier and Mason, 1984), provide stable platforms for instrumentation but have limited portability because of their size. Furthermore, crawler vehicles and other seabed-contact platforms are unsuitable for coral reefs and rocky shores, where their operation may damage fragile benthic communities.

Acoustic methods remain one of the most reliable approaches for direct bathymetric measurement in energetic nearshore environments. Sonar altimeters have been shown to perform in bubbly water (Gallagher et al., 1996), where optical methods fail, and remain effective under rough sea conditions (Forte et al., 2026). Nevertheless, conventional boat-based sonar surveys are often impractical or unsafe in shallow, energetic surf zones (Work et al., 1998). Other floating platforms, such as kayaks, can access shallower water but are difficult to maneuver in breaking waves (e.g., Mead and Black, 2001; Kimball et al., 2014). Personal watercraft (jet skis) equipped with sonar altimeters are widely used for surf zone bathymetric surveys and are considered the current standard for in-situ measurements (e.g., Dugan et al., 2001; Lippmann and Smith, 2009; MacMahan, 2001; Moulton et al., 2014). GNSS (Global Navigation Satellite System) based corrections that provide wave corrections and bathymetric measurements to a fixed vertical datum are used in some contemporary jet ski survey systems (e.g., Dugan et al., 2001). However, these jet skis typically require permits, trailer transport, and launch site access, limiting their portability and ease of deployment. Jet skis also cannot be operated safely in areas with high densities of beachgoers such as swimmers and surfers because of their impellers and potential for collision. As a result, safely deploying acoustic sensors while maintaining portability and the ability to survey highly dynamic nearshore environments remains a challenge.

Here, we present the *BathyBoard*, a low-cost, portable surfboard-based platform equipped with a sonar echo sounder and GNSS receiver for measuring nearshore bathymetry. Surfboards are highly maneuverable in breaking waves and have been used to collect in-situ measurements of water properties and constituents (e.g., Bresnahan et al., 2022; Brewin et al., 2015; Camins et al., 2020), but have not previously been adapted for bathymetric surveying. We begin by discussing the platform components and data processing procedures.

Field validation of the *BathyBoard* is then presented, and a repeatability test is conducted. Measurement differences in sources, as well as *BathyBoard* benefits and limitations are discussed. A summary of the *BathyBoard* capabilities for nearshore bathymetry surveying is provided.

METHODS

Platform Components

The *BathyBoard* is a low-cost, portable bathymetric surveying platform built around a surfboard equipped with a GNSS receiver and echo sounder (Fig. 1). The platform is based on a Prodonavich-shaped longboard surfboard, measuring 8′10” × 22.5” × 3.25” (length × width × thickness). The board serves as a stable platform for carrying the survey instrumentation while maintaining sufficient maneuverability for operation within the surf zone. All board movement is powered by the operator through paddling. Paddle speed is approximately 1.5 m/s, but varies with paddling skill. For operator safety and equipment retention, the board is attached to the surveyor using a standard surf leash.

Bathymetric measurements are collected using an Echologger EA400 single-beam echo sounder. The echo sounder operates at a fixed acoustic frequency of 450 kHz with a 5° conical beam and was sampled at 10 Hz, yielding dense along-track coverage with a sounding interval of approximately 0.15 m at the typical survey speed. In addition to water depth, the EA400 records pitch and roll. To ensure synchronization between sensors, the echo sounder clock was synchronized to laptop internet time immediately prior to each survey. Although the absolute synchronization accuracy is unknown, it is expected to be better than one second, and clock drift during individual surveys was assumed to be negligible.

Positioning is provided by an Emlid Reach M2 GNSS receiver operating at 10 Hz with a satellite masking angle of 30°. The GNSS receiver antenna and echo sounder transducer are aligned vertically within a custom instrument tower to reduce horizontal offsets between the positioning and depth measurements (Fig. 1). A cylindrical hole was drilled through the surfboard and sealed with fiberglass and resin, allowing the transducer housed within the tower to be mounted flush with the board’s underside to minimize flow disturbance caused by the instrument. The tower is positioned near the rear of the board between the operator’s legs (Fig. 1e) and consists of a 3-in. diameter flange attached to the deck of the board around the hole, a 10-in. long vertical threaded PVC (polyvinyl chloride) pipe, a threaded connecting rod used to secure the echo sounder within the pipe, a 3-in. diameter aluminum ground plane supporting the GNSS antenna, and a 3-in. diameter PVC cap at the top of the tower to contain the components. The vertical separation between the GNSS receiver

antenna phase center and the echo sounder transducer is 0.3 m. The instrument tower is additionally secured to the board leash plug with a safety tether to prevent equipment loss during operation.

The operator navigates using an Oukitel RT5 rugged tablet (IP68-rated waterproof) housed within a secondary waterproof Pelican case mounted externally on the nose of the board. The tablet displays planned survey tracks in real time while simultaneously recording its position using its internal GNSS receiver. Although the receiver provides sufficient accuracy for navigation, its vertical and horizontal positioning error is on the order of meters to tens of meters and is therefore not used for bathymetric measurements. The operator is provided with continuous feedback on position, elapsed survey time, and distance traveled, facilitating efficient coverage of the survey area and adherence to predetermined survey lines. The complete *BathyBoard* system costs approximately $7,000 USD and can be deployed and operated by a single user. The largest expense is the Echologger EA400 echo sounder ($5,000), followed by the Emlid Reach M2 GNSS receiver and antenna ($1,023). The remaining components account for less than $1,000 of the total system cost.

Data Processing

Echo Sounder

The raw echogram from each survey was processed using a threshold-based bottom-detection algorithm. Threshold-based bottom detection is widely used in single-beam echo sounders because the seabed typically produces the strongest acoustic backscatter in the water column (e.g., Bourguignon et al., 2009). For each acoustic ping, a dead zone and amplitude threshold were defined. The dead zone defines a near-field blanking distance over which acoustic returns are ignored, while the amplitude threshold defines the minimum signal amplitude considered a valid bottom return. For each ping, the depths beyond the dead zone of the first, maximum-amplitude, and last returns exceeding 20% of the full scale (maximum measurable signal amplitude) were identified as candidate bottom depths. The mean depth of the pair (first-max or max-last) exhibiting the smallest depth variance was used as a bottom estimate. If the pairs had the same variance, the mean depth of the first-max pair was used as the bottom estimate.

Orientation Corrections and Quality-Control

Pitch and roll motions of the *BathyBoard*, measured by a ±90° dual-axis tilt sensor with 0.1° accuracy, alter both the orientation of the echo sounder beam and the relative position of the GNSS receiver antenna and transducer. Orientation corrections were therefore applied to all observations. The measured echo

sounder depth was projected onto the vertical, assuming a flat bottom, with a similar method as Work et al. (1998) using the observed pitch (θ) and roll (ϕ) angles,

$$h_c = h\cos(\theta)\cos(\phi) \tag{1}$$

where h and h_c are the measured and corrected depths, respectively. To identify observations collected during periods of excessive platform motion, a sensor tilt angle α was computed as

$$\alpha = \cos^{-1}(\cos\theta\cos\phi) \tag{2}$$

Observations with $\alpha > 15°$ were removed and replaced by linear interpolation between neighboring measurements, as the assumptions underlying the beam-angle correction (e.g., a locally flat bottom) become less reliable at larger sensor tilts. This corresponded to removing $0.86 - 2.28\%$ of the points, depending on the survey. The threshold for α (15°) was selected after preliminary testing over a range of values across various sites. This is similar to the 10° pitch and roll threshold used by Forte et al. (2026) to remove high tilt points. Because the GNSS antenna was mounted a distance 0.3 m directly above the echo sounder transducer, GNSS elevations were also adjusted to estimate the elevation of the transducer. Using the measured pitch and roll angles from the echo sounder tilt sensor, the vertical antenna to transducer separation was computed as $0.3\cos\alpha$ m. Together, these corrections account for tilt-induced changes in both the echo sounder measurement geometry and the vertical separation between the GNSS antenna and transducer, ensuring that the depth and elevation measurements are referenced consistently.

GNSS Corrections and Vertical Referencing

The GNSS receiver tracked multiple constellations, including the Global Positioning System (GPS), Russian Global Navigation Satellite System (GLONASS), Galileo, Quasi-Zenith Satellite System (QZSS), BeiDou Navigation Satellite System, and Indian Regional Navigation Satellite System (IRNSS), and produced position data in Receiver Independent Exchange Format (RINEX), time-stamped in Coordinated Universal Time (UTC). Local time during the California surveys was Pacific Daylight Time (PDT; UTC−7), whereas on O‘ahu, it was Hawai‘i Standard Time (HST; UTC−10). The rover (Reach M2) coordinates associated with the RINEX observations were initially expressed in the World Geodetic System 1984 (WGS 84) coordinate system and then subsequently processed using Post-Processed Kinematic (PPK) techniques in Emlid Studio.

The rover observations were processed relative to either a permanent Trimble NetR9 base-station atop the Center for Coastal Studies building at Scripps Institution of Oceanography (SIO) for the California surveys or a temporary Emlid Reach RS2 base-station for the Hawai‘i surveys. All base-station observations were processed using the National Oceanic and Atmospheric Administration (NOAA) Online Positioning User Service (OPUS), yielding coordinates referenced to the North American Datum of 1983 realization fixed to the North American tectonic plate [NAD 83(2011)], epoch 2010.00, for the San Diego surveys and the corresponding realization fixed to the Pacific tectonic plate [NAD 83(PA11)], epoch 2010.00, for the Hawai‘i surveys. During PPK processing, the corrected rover coordinates inherited the reference frame of the corresponding base-station coordinates. Only fixed PPK solutions were retained for analysis, while float and single solutions were discarded to ensure the highest possible positioning quality. Fixed solutions accounted for more than 90% of the epochs across all surveys. According to the manufacturer's specifications, the Reach M2 provides kinematic positioning accuracies of 7 mm ± 1 ppm horizontally and 14 mm ± 1 ppm vertically when operating with a fixed solution. Ellipsoidal heights were converted to orthometric heights referenced to the North American Vertical Datum of 1988 (NAVD 88) using the GEOID 12B geoid model. The orthometric heights were subsequently transformed to elevations relative to local Mean Sea Level (MSL), by applying a constant datum offset obtained from NOAA's published tidal datums at the nearest tide station to each survey site. MSL served as the vertical datum for the bathymetric measurements.

Additional corrections were required to account for variations in the water-surface elevation through time. Since the *BathyBoard* operates in the surf zone, instantaneous water depths measured by the echo sounder are influenced by the tide and wave-induced fluctuations of the free-surface. When the platform is located on a wave crest, the measured depth is greater than the depth that would be observed relative to a still-water surface. Conversely, when the platform is located within a wave trough, the measured depth is reduced. Small (< 1 s) timing offsets between the echo sounder and GNSS measurements due to limited internet time synchronization precision, were estimated by maximizing the cross-correlation between the records and corrected by shifting the echo sounder time series accordingly. To remove the influence of free-surface fluctuations, the GNSS-derived, low-pass filtered (0.5 Hz cutoff frequency) elevation of the platform relative to MSL was combined with the echo sounder depth measurement to determine the bed elevation relative to the datum. Since the GNSS receiver antenna was mounted directly above the echo sounder transducer, both sensors experienced nearly identical heave motions, allowing the wave-induced vertical displacement to be removed directly through the GNSS receiver elevation record. This procedure yields bathymetric

measurements referenced to a fixed vertical datum rather than to the instantaneous free-surface. Further details are described in the following "Sea-Swell Wave Signal Removal" section.

RESULTS

Sea-Swell Wave Signal Removal

In this section, we evaluate the ability of the Emlid Reach M2 GNSS receiver to remove wave-induced free-surface fluctuations from the EA400 echo sounder measurements, as outlined in "GNSS Corrections and Vertical Referencing". A stationary field test was conducted approximately 250 m offshore of Scripps Beach in California (Fig. 2), where shoaling waves propagated over a sandy seabed. During the test, the board operator maintained the *BathyBoard* at an approximately fixed location, assumed to have constant local bathymetry, for four minutes (17:09–17:13 UTC, July 03, 2024). Meteorological conditions were calm, with light texture on the water surface. An anemometer mounted on Scripps Pier measured winds of 1.6 m/s from the north-northwest (336°) and gusts up to 3.0 m/s. Wave conditions from the Coastal Data Information Program (CDIP) Scripps Nearshore Buoy indicated a significant wave height of $H_s = 0.9$ m and peak period of $T_p = 9$ s. The tilt quality-control procedure removed 0.86% of observations. The power spectra of the tilt corrected and quality-controlled echo sounder depth fluctuations, $Z'_S = Z_S - \bar{Z}_S$, and GNSS elevation fluctuations, $Z'_G = Z_G - \bar{Z}_G$, were estimated using Welch's method (Welch, 1967) with a Hanning window, 50% overlap between 40 s segments, and approximately 16 degrees of freedom. The resulting spectra are very similar within the sea-swell (SS) frequency band (0.05–0.5 Hz), indicating that both sensors are responding to the same wave-induced motions (Fig. 3a).

Both signals contain a spectral peak in the SS band at 0.10 Hz, which agrees well with the peak frequency measured by the Scripps Nearshore Buoy (0.11 Hz). The similarity between the two spectra is further reflected in the high magnitude-squared coherence (MSC) between the two in the SS band, with an average MSC of 0.88 ± 0.10 (Fig. 3b). Across the SS band, the phase increases quasi-linearly from near 0° at $f = 0.05$ Hz to near 50° at $f = 0.5$ Hz (Fig. 3c). Linear phase variation is consistent with a constant time lag between the echo sounder and the GNSS measurements and is estimated to be ≈ 0.3 s between 0.1–0.5 Hz. Cross-correlation between Z'_S and Z'_G (Fig. 4a) was highest ($r = 0.79$) at a lag of ≈ 0.2 s, compared with $r = 0.76$ at zero lag. This small difference indicates that the lag has little effect on the wave-correction procedure. Nevertheless, the echo sounder time series was shifted in all analyses to maximize its correlation with the GNSS heave. The source of this lag is unknown but may be attributable

to small clock drift or, more likely, uncertainty in the initial synchronization between the echo sounder and laptop internet time. The strong coherence and similar spectral structure within the SS band indicate that both sensors capture a common wave-induced signal (Fig. 3a,b). At frequencies greater than 0.5 Hz, the spectra begin to diverge. The GNSS spectrum exhibits greater energy than the echo sounder in this high-frequency range, while coherence decreases substantially to 0.18 ± 0.15. This behavior suggests that the GNSS signal contains additional high-frequency noise that is not present in the echo sounder measurements. Accordingly, a low-pass filter with a cutoff frequency of 0.5 Hz was applied to the GNSS elevation record prior to wave correction. This removes high-frequency GNSS noise while retaining the dominant sea-swell motions responsible for free-surface fluctuations.

The effectiveness of this approach was evaluated using the four-minute stationary test shown in Fig. 4b, with the time lag correction applied to the echo sounder data. Prior to wave correction, the mean echo sounder depth was 6.63 ± 0.20 m, here referred to as the raw transducer to bottom distance and not referenced to a vertical datum. After applying the wave correction by subtracting the low-pass filtered GNSS elevation fluctuations, $\tilde{Z}'_G$, the mean depth was 6.60 ± 0.07 m, indicating little change in the mean depth while substantially reducing wave-induced variability. The standard deviation decreased by approximately 65%, compared to a reduction of only 40% when the unfiltered GNSS elevation fluctuation signal was used. For this demonstration, only the fluctuating component of the low-pass filtered GNSS elevation was removed from the echo sounder depth. Referencing the measurements directly to MSL (as done in the "Jet Ski Based Sonar Comparison at a Sandy Beach" and "Aerial LiDAR Validation at Coral Reef Sites" results sections) would require subtracting the full low-pass filtered GNSS elevation, $\tilde{Z}_G$, which would introduce a constant depth offset into the stationary comparison in Fig. 4b. The fluctuation-only correction isolates the effectiveness of the wave-removal procedure without altering the mean depth. The low-pass filtered GNSS elevation fluctuations, $\tilde{Z}'_G$, and echo sounder depth fluctuations, Z'_S, were strongly correlated ($r = 0.95$), confirming again that both sensors respond to the same wave-induced motions (Fig. 4c). A linear regression between the two signals yielded a slope of 0.86, indicating that the magnitude of the fluctuations recorded by the echo sounder was slightly smaller than that of the fluctuations measured by the GNSS receiver.

Potential sources of discrepancy between Z'_G and Z'_S were therefore examined. One possible source of error is sensor tilt, which can introduce noise into *BathyBoard* observations. The mean tilt angle (2) was $\alpha = 1.13 \pm 0.62°$, with a maximum value of 5.1°. No relationship was observed between large values of α and outliers in the GNSS–echo sounder comparison (Fig. 4c), indicating that platform pitch and roll corrections

were not a primary source of error. Similarly, the standard deviation of the platform displacement from its mean position, $\mathbf{X}'$, was 0.54 m, with a maximum displacement of 2.4 m, reflecting modest drift due to waves and currents during the stationary test. No relationship was observed between increased displacement and outlier measurements (not shown), suggesting that horizontal platform motion also had a negligible influence on the comparison. The reduction in depth variance following wave correction, and the strong correlation between the GNSS and echo sounder signals, demonstrates the effectiveness of the *BathyBoard* configuration for removing wave-induced free-surface fluctuations from bathymetric measurements. The wave correction procedure described above was therefore applied to all subsequent analyses.

Jet Ski Based Sonar Comparison at a Sandy Beach

Within this section, *BathyBoard* bathymetric measurements are compared against surveys collected using the SIO Coastal Processes Group's sonar-equipped jet ski, a well-established platform for nearshore bathymetric surveying that has been used extensively in coastal research (e.g., Lange et al., 2023; Ludka et al., 2015, 2018, 2019; Seymour et al., 2005; Yates et al., 2009). The current jet ski is a 2025 Yamaha GP HO™ with a custom designed single-beam echo sounder and a Trimble NetR9 GNSS receiver. The echo sounder is mounted near the aft of the jet ski and operates at 192 kHz with a 20° beam width, sampling at 20 Hz. The GNSS receiver records positions at 5 Hz and receives real-time kinematic (RTK) corrections from a Pacific Crest radio modem operating at 464.75 MHz. Vessel heave corrections and vertical datum referencing are performed using GNSS measurements, while pitch and roll corrections are applied to both the measured depth and horizontal position using the echo sounder tilt sensor. Survey navigation is supported by custom data acquisition and visualization software running on a Panasonic Toughpad rugged tablet. The jet ski surveys at higher speeds than the *BathyBoard*, typically 2–5 m/s compared to an average paddling speed of approximately 1.5 m/s, and can operate continuously for roughly four hours on a single tank of fuel. These capabilities enable rapid surveying of large coastal areas. The total cost of the jet ski survey system is approximately $\$80,000$.

Concurrent surveys using the *BathyBoard* and the bathymetry jet ski were conducted along two cross-shore Monitoring and Protection (MOP) transects (510 and 512) (O'Reilly et al., 2016), located just south of Scripps Pier (Fig. 5a,b). The transects are separated by approximately 200 m in the alongshore direction (black lines in Fig. 5c,d). During the surveys, the water-level from the NOAA Scripps Pier tide gauge was 0.31 m above mean sea level (MSL). The Scripps Nearshore CDIP buoy recorded a significant wave height

of $H_s = 0.92$ m and peak period of $T_p = 8.33$ s throughout the survey. The tilt quality-control procedure resulted in the removal of 0.95% of *BathyBoard* measurements. Both platforms successfully collected bathymetric measurements from the surf zone out to water depths of nearly 10 m. However, the *BathyBoard* was able to operate in shallower water than the jet ski owing to its shallow draft and maneuverability within the surf zone. This is evident in Fig. 5a,b, where the *BathyBoard* survey tracks extend farther onshore than those of the jet ski. The shallowest bed elevation measured by the *BathyBoard* was −0.05 m MSL, compared with −1.14 m MSL for the jet ski. As a result, the *BathyBoard* provided bathymetric coverage closer to the shoreline and within actively breaking waves, where conventional survey vessels are more limited and bathymetry is generally collected from shore using GNSS surveys at low tide.

For comparison, all bathymetric observations were transformed into a local SIO coordinate system. The coordinate origin was defined at the base of Scripps Pier (red circle in Fig. 5a), with $-X_{\mathrm{SIO}}$ directed offshore along the pier axis and $-Y_{\mathrm{SIO}}$ directed southward along the coastline. The transformed *BathyBoard* and jet ski measurements are shown in Fig. 5c,d, respectively. Deviations from the prescribed survey line were necessary for the *BathyBoard* along MOP 510 around $X_{\mathrm{SIO}} = -110$ m to avoid breaking waves within the surf zone. Survey-line adherence was quantified by comparing the measured tracks to the corresponding MOP transects. The mean distance between each observation and the nearest point on the corresponding MOP transect, ΔMOP, was 4.5 ± 2.8 m for the *BathyBoard* and 1.1 ± 0.8 m for the jet ski. The larger deviations observed for the *BathyBoard* are attributable to the difficulty of maintaining precise survey-line tracking while paddling in energetic wave conditions. This challenge is further compounded by the *BathyBoard* tablet's internal GNSS receiver, which is used for real-time navigation and provides only meter- to tens-of-meter-level positioning accuracy.

For both the *BathyBoard* and jet ski datasets, bathymetric observations were projected onto the cross-shore MOP transects. The resulting profiles along MOP 512 and 510 show excellent agreement between the two survey platforms (Fig. 6a,b). Because the *BathyBoard* was able to survey in shallower water than the jet ski, a direct comparison was restricted to regions sampled by both platforms. Accordingly, *BathyBoard* observations were clipped to the cross-shore transect extent of the jet ski data prior to calculating agreement statistics. A k-nearest neighbors (KNN) search was then used to pair each retained *BathyBoard* observation with its nearest jet ski measurement in Universal Transverse Mercator (UTM) coordinates. The matched bathymetric elevations agree closely, with a correlation of $r = 0.998$ and a root-mean-square difference (RMSD) of 0.14 m (Fig. 6c), comparable in magnitude to errors reported in previous surf

zone survey system validation studies (e.g., Bak et al., 2023; Forte et al., 2026; MacMahan, 2001). The mean horizontal separation distance between KNN-matched observations $\Delta|\mathbf{X_m}|$ was 4.81 ± 3.01 m, with a maximum separation of 12.08 m (Fig. 5). Larger separation distances generally occurred near the middle of the transects, where the *BathyBoard* tracks deviated more from the prescribed MOP lines than the jet ski. Despite these deviations, no increase in residual scatter was observed with increasing separation distance. This suggests that bathymetric variability in the alongshore direction was small over the spatial scales considered, allowing robust comparison between the two datasets despite imperfect spatial overlap.

Repeat-Pass Vertical Uncertainty

BathyBoard measurement repeatability was evaluated using 20 cross-shore passes collected north of the Scripps Pier ($+Y_{\mathrm{SIO}}$), comprising 10 offshore-directed and 10 onshore-directed passes over approximately the same transect. Coordinates were transformed into the SIO reference frame described in the Jet Ski-Based Sonar Comparison section, and each elevation profile was linearly interpolated onto a common 1 m grid in the X_{SIO} direction. During the survey, the CDIP Scripps Nearshore Buoy recorded small, short period swell, with $H_s = 0.45$ m and $T_p = 8.3$ s. Bathymetry measurements were consistent among the 20 passes, each spanning 70 m in the cross-shore direction (X_{SIO}) (Fig. 7a). Elevation residuals were calculated relative to the median of the repeated-pass measurements at each cross-shore grid location (Fig. 7c). The mean absolute residual across all profiles was 0.029 ± 0.022 m, indicating close agreement among repeated measurements. The horizontal survey positions were also well reproduced (Fig. 7b), with a mean alongshore position of $Y_{\mathrm{SIO}} = 141.8 \pm 0.9$ m across all passes. The onshore-directed passes were generally located slightly farther north than the offshore-directed passes, as indicated by their higher Y_{SIO} values. This systematic offset resulted from the direction in which the operator rounded the marker float when reversing course.

Following Bak et al. (2023), the repeat-pass total vertical uncertainty (TVU) at each cross-shore location was estimated at the 95% confidence level as

$$\mathrm{TVU}(X_{\mathrm{SIO}}) = 1.96\,\sigma_{Z_{\mathrm{MSL}}}(X_{\mathrm{SIO}}), \tag{3}$$

where $\sigma_{Z_{\mathrm{MSL}}}$ is the standard deviation of the 20 interpolated bathymetry measurements at that location. The resulting TVU was low and relatively uniform along the transect, with a cross-shore mean of 0.072 ± 0.012 m (Fig. 7d). This uncertainty is comparable to that reported for repeated surf zone surveys conducted with an amphibious crawler (Bak et al., 2023). Neither the elevation residuals nor the TVU exhibited a clear

dependence on the variability in alongshore position, $\sigma(Y_{\mathrm{SIO}})$ (Fig. 7c,d), likely because the bathymetry was relatively alongshore uniform. Both quantities also remained approximately constant with X_{SIO}, indicating little dependence of repeatability on water depth or cross-shore position. Notably, the onshore portion of the transect extended into a region of steep, shoaling waves, where platform tilt and wave-induced vertical motion were greater. The consistently low uncertainty indicates that the *BathyBoard* produced repeatable bathymetry measurements across variations in travel direction, platform orientation, wave phase, and measurement time.

Aerial LiDAR Validation at Coral Reef Sites

Next, we evaluate the *BathyBoard's* ability to map coral reef bathymetry at two sites on O'ahu, Hawai'i. Bathymetric measurements were compared against a topobathymetric aerial LiDAR dataset collected by the United States Army Corps of Engineers (USACE) in 2013 with an estimated point spacing of 0.35 m. Both sites, Kewalos (Fig. 8b) and Kaiser's (Fig. 8c), are well-known surf breaks along the south shore of O'ahu (Fig. 8a). Each site is adjacent to a harbor channel (Kewalos to the west and Kaiser's to the east). The Kewalos survey primarily focused on the reef region and did not cover the channel, while the Kaiser's survey did include the channel. The Kewalos survey was more irregular and did not follow a uniform grid, due to the operator having to navigate breaking waves and surfers (Fig. 8b). A jet ski based survey would be difficult to conduct safely at these sites because of the density of swimmers and surfers. Additional sampling density was obtained in the wave-breaking region. Sporadic breaks in lines are due to degraded GNSS reception as a result of waves breaking over the receiver. As a result, approximately 10% of observations were removed during GNSS quality-control filtering at Kewalos. The tilt quality-control procedure resulted in the removal of 2.28% of observations at Kewalos and 1.90% at Kaiser's. The Kaiser's survey was collected by first outlining a bounding box, followed by repeated passes in a lawnmower pattern with approximately 25 m spacing, conducted in both cross-shore and alongshore directions, with more coverage in the cross-shore direction directly in the active wave breaking region (Fig. 8c).

A KNN search was used to associate each *BathyBoard* sonar observation with the nearest point in the aerial LiDAR dataset. This approach reduces the higher-resolution LiDAR dataset to a subset of points directly comparable to the *BathyBoard* measurements, enabling point-by-point evaluation of bathymetric agreement. Prior to outlier removal, the mean absolute horizontal separation distance between matched *BathyBoard* and LiDAR observations was 0.40 ± 0.73 m at Kewalos and 0.34 ± 0.24 m at Kaiser's. To minimize mismatches caused by interpolation across widely separated survey tracks, matched pairs with

horizontal separation distances greater than 1 m were excluded from the analysis. This filtering removed a small percentage of observations (3.4% at Kewalos and 1.8% at Kaiser's), yielding mean absolute horizontal separation distances of 0.31 ± 0.18 m and 0.32 ± 0.19 m, respectively. Sensitivity analyses using separation thresholds ranging from $1 - 3$ m produced nearly identical error statistics at both sites, indicating that the comparison metrics were not strongly influenced by the selected threshold.

A two-dimensional (2-D) histogram comparing the *BathyBoard* and aerial LiDAR matched depths shows that the majority of observations were tightly clustered about the one-to-one line (Fig. 9). At Kewalos and Kaiser's, 83% and 89% of matched observations, respectively, fell within ±0.5 m of the one-to-one line, indicating strong agreement between the *BathyBoard* and LiDAR measurements. The binned means, computed in 0.5 m intervals of Aerial LiDAR Z_{MSL}, deviated from the one-to-one line by an average of 0.41 m at Kewalos and 0.11 m at Kaiser's. The mean binned standard deviation was 0.52 m at Kewalos and 0.37 m at Kaiser's, with maximum values of 0.84 m and 0.61 m, respectively, occurring at greater depths. At Kewalos, agreement between the *BathyBoard* and LiDAR measurements decreased with increasing water depth, whereas at Kaiser's the agreement showed less dependence on depth. The Kewalos comparison yielded a high correlation coefficient of $r = 0.93$, RMSD of 0.45 m, and a linear regression slope of 0.91 (Fig. 9a). Agreement was even stronger at Kaiser's, where $r = 0.98$, the RMSD was 0.34 m, and the regression slope was 0.95 (Fig. 9b). These results demonstrate that the *BathyBoard* successfully reproduces the overall bathymetric structure measured by airborne LiDAR across a range of nearshore depths and bottom morphologies.

DISCUSSION

Sources of Measurement Differences

Although agreement was generally strong, several factors likely contribute to the discrepancies between the *BathyBoard* measurements and those obtained from the jet ski (Fig. 6) and airborne LiDAR (Fig. 9) surveys. First, clock drift and timing offsets between the GNSS receiver and echo sounder on the *BathyBoard* can reduce the effectiveness of the wave correction. Because the correction relies on synchronizing water-level fluctuations from independently initialized GNSS and echo sounder time series, small timing offsets can introduce uncertainty into individual depth estimates. Although cross-correlation and interpolation onto a common time base improved alignment between the independently recorded GNSS and echo sounder measurements, residual clock drift or time-varying synchronization errors may remain. These residual offsets

may contribute to uncertainty in the wave correction procedure, particularly during periods of elevated wave activity when vertical motions of the platform are largest.

Temporal separation between surveys contributed to differences between the *BathyBoard* and airborne LiDAR datasets collected on O'ahu. The LiDAR surveys preceded the *BathyBoard* measurements by approximately a decade. Although major geomorphic features of the reef platform likely remained stable over this period, smaller-scale morphology may have evolved due to biological growth, wave damage, and coral mortality associated with ocean warming (Hughes et al., 2018). Consequently, some discrepancies likely reflect genuine changes in seafloor morphology rather than measurement error alone. These factors suggest that differences between datasets should not be interpreted only as measurement uncertainty.

A portion of the observed differences between the *BathyBoard* and LiDAR datasets is expected to arise from uncertainty in the LiDAR measurements themselves. The reported accuracy of the bathymetric LiDAR data from USACE is depth dependent and specified at the 95% confidence level. The vertical accuracy is given by $\sqrt{0.25^2 + (0.0075h_l)^2}$ m, where h_l is the LiDAR water depth in meters. The corresponding horizontal accuracy is $3.5 + 0.05h_l$ m. At representative water depths of 2 m and 6 m, these specifications correspond to vertical uncertainties of approximately 0.250 m and 0.254 m, respectively, and horizontal uncertainties of 3.6 m and 3.8 m. Horizontal position errors can result in points being associated with neighboring bathymetric features rather than their true counterparts in the KNN search, thereby introducing additional scatter into the comparison. This effect is expected to be most pronounced in regions with steep bathymetric gradients, where small horizontal offsets can correspond to substantial differences in water depth. This may explain the greater deviations in agreement between the *BathyBoard* and LiDAR at deeper depths, particularly for the Kewalos case.

Benefits and Future Improvements

The *BathyBoard's* primary advantage over jet ski based surveying systems is its cost, portability, ease of deployment, and ability to operate safely in locations with swimmers and surfers, while maintaining comparable bathymetric accuracy. The platform can be transported on commercial flights to remote locations and launched from nearly any shoreline, allowing bathymetric surveys in areas where other survey approaches may be logistically challenging or prohibitively expensive. Unlike jet ski based systems, operation does not require fuel, trailers, launch ramps, or specialized permitting, and can often be conducted with minimal disruption to other coastal users such as surfers or swimmers. The platform can also maneuver through

extremely shallow water and actively breaking waves, enabling surveys in regions that are often difficult to access using larger survey systems. Compared with costly and infrequent airborne LiDAR surveys, the low-cost, portable *BathyBoard* enables rapid, on-demand surveys and can expand access to surf zone bathymetric mapping for research groups and coastal communities. Its human-powered, non-contact design also makes it suitable for surveying environmentally sensitive habitats such as coral reefs and rocky shorelines, where seabed contacting vehicles may be undesirable. These characteristics fill an important observational gap between large-scale remote sensing techniques and other in-situ nearshore survey systems. The *BathyBoard* is currently used by multiple researchers within the Coastal Processes Group at SIO for targeted nearshore studies, despite the availability of a survey jet ski. Its shallow draft, portability, and rapid deployment make it better suited to small surf zone areas where mobilizing a jet ski may be inefficient or operationally impractical, demonstrating its value as a complementary survey platform. Because it uses commercially available components, the documented system design and processing workflow can also be reproduced or adapted by other groups.

Although we have shown that the *BathyBoard* can reliably collect nearshore bathymetry in energetic surf zone environments over both sand and reef bottoms, several limitations were identified during system development and field deployments that point to future *BathyBoard* improvements. The *BathyBoard* is less suitable for large area hydrographic surveys, where conventional platforms can cover ground more efficiently, and is instead intended to complement these methods in targeted, shallow surf zone applications. Safe operation of the *BathyBoard* requires proficiency in surf zone surfboard handling and sufficient endurance for extended paddling. Surveys are therefore conducted as part of a field team under a site specific safety plan, with shore-based personnel providing support. Deployment is constrained by site access and conditions, including wave shape and energy, currents, the presence of shallow rocks or reefs, and remoteness, which may preclude safe operation. Before each deployment, the field team should conduct a structured risk assessment and final go/no-go evaluation. For example, the NOAA Green-Amber-Red (GAR) operational risk assessment framework provides an adaptable method for evaluating resources, environmental conditions, team experience, personnel fitness, and mission complexity (e.g., National Oceanic and Atmospheric Administration, 2020). Paddling and flow around the echo sounder may create turbulence and entrained air beneath the board, which could degrade the acoustic return. The deck mounted PVC tower used to position the echo sounder and GNSS receiver creates a large physical footprint between the user's legs and interferes with movement. Integrating system components directly into the board would further enhance stability and

reduce system complexity. Utilizing a smaller echo sounder within a molded recess in the foam core would eliminate the need for an external tower mount and ensure consistent sensor alignment. This would also significantly lower the price of the system, as the current echo sounder makes up approximately 70% of the total cost. A lower-cost echo sounder such as the Cerulean Sonar Sounder S500 is available for approximately \$890, which would reduce the total platform cost to less than $\$3,000$.

Aspects of data acquisition and synchronization could also be improved. In the current configuration, GNSS receiver and echo sounder data streams are recorded independently and must be aligned in post-processing, introducing potential timing errors. Implementing synchronized triggering of all instruments would eliminate these alignment issues and improve overall data quality. Furthermore, the use of PPK GNSS limits situational awareness during surveys because positioning quality cannot be fully assessed until post-processing. RTK positioning would allow operators to evaluate positioning accuracy in real time and adapt the survey strategy accordingly. However, RTK would require additional radio hardware or, alternatively, a reliable cellular or network connection to receive Networked Transport of RTCM via Internet Protocol (NTRIP) corrections. These requirements would increase system complexity and could limit operation in remote areas. RTK may also be less robust than PPK when correction communications are intermittent, potentially reducing positioning availability or accuracy. Finally, the lack of real-time feedback on platform attitude and data quality limits operational control. Incorporating onboard visualization of yaw, pitch, roll, and heave, as well as embedding the tablet display directly into the board, would provide immediate feedback to the user. This would encourage more consistent survey execution by helping operators maintain even weight distribution and avoid excessive board tilt, while also allowing periods of excessive motion or potentially poor data quality to be identified during collection rather than after the fact. Together, these improvements would increase measurement accuracy and reduce system complexity, resulting in a more robust *BathyBoard* platform for nearshore bathymetric surveying.

SUMMARY

This study presents the *BathyBoard*, a low-cost bathymetric survey platform designed to map shallow nearshore and surf zone waters that are difficult to survey using existing survey methods. The platform integrates an Echologger EA400 echo sounder and an Emlid Reach M2 GNSS receiver on a surfboard-based platform, with a total system cost of approximately \$7,000. A GNSS-based wave correction methodology was used to remove wave-induced free-surface fluctuations from the echo sounder measurements. Spectral

analysis demonstrated strong agreement between GNSS elevation fluctuations and echo sounder depth fluctuations within the sea-swell frequency band. Application of the wave correction reduced the standard deviation of measured water depths by 65%. The accuracy of the *BathyBoard* was evaluated through comparisons with two independent bathymetric datasets. Comparison with a sonar-equipped survey jet ski along established cross-shore MOP transects near Scripps Pier showed excellent agreement, with a correlation of 0.998 and RMSD of 0.14 m, comparable to the accuracy of other surf zone surveying systems (e.g., Bak et al., 2023; Forte et al., 2026; MacMahan, 2001). While the jet ski followed prescribed survey lines more precisely, the *BathyBoard* successfully collected measurements in appreciably shallower water due to its greater maneuverability within the surf zone. Ten out-and-back *BathyBoard* repeat passes of a cross-shore transect produced a mean total vertical uncertainty (4) of 0.072 m, demonstrating consistent measurements across different survey directions. Additional validation was performed at two coral reef sites on the south shore of Oʻahu, using bathymetric aerial LiDAR data collected by the USACE. The *BathyBoard* showed strong agreement with the LiDAR data at both sites, with correlations of 0.93 and 0.98 and RMSDs of 0.45 m and 0.34 m at Kewalos and Kaiser's, respectively. The strong agreement with the independent jet ski and aerial LiDAR datasets demonstrates that the *BathyBoard* provides an effective and inexpensive approach for collecting high-resolution bathymetry in shallow coastal environments. Because the platform is portable, can be transported on commercial flights to remote locations, launched directly from shore without a ramp, is entirely human-powered, and is capable of operating within actively breaking waves, it fills an important observational gap between traditional vessel-based surveys and remote sensing techniques. The simplicity and affordability of the *BathyBoard* may broaden participation in coastal surveying by enabling high-resolution bathymetric measurements in environments that have been historically data-sparse.

Data Availability Statement

All data and code that support the findings of this study are available from the corresponding author upon reasonable request.

Acknowledgments

We appreciate the support provided by the Mark Walk Wolfinger Foundation to make this research possible. K. Pick was supported by the Mark Walk Wolfinger Foundation. K. Quinn was supported by an ORISE (Oak Ridge Institute for Science and Education) Fellowship. N. Cirrito was funded by a NOAA (National Oceanic and Atmospheric Administration) SCCOOS (Southern California Coastal Ocean

Observing System) IRA (Inflation Reduction Act) award number UDR0000654. A. Domi was supported by the University of California San Diego Regents Fellowship, USACE award number W912HZ-24-2-0035, and the California Department of Parks and Recreation Natural Resources Division Oceanography Program C19E0026. We are grateful to Brian Woodward of the Coastal Processes Group field crew for collecting jet ski nearshore bathymetry. We thank NOAA and the USACE for providing publicly available aerial LiDAR bathymetry and NOAA for providing the coastal DEM data. Additional *BathyBoard* survey help from Andrew Davey and Brennan Kimura was much appreciated. Discussions with Brian Woodward, Rob Grenzeback and Matthew Spydell were valuable in informing data processing methods. Help with board outfitting was provided by Joe Roper's Surfboard Repair, Kent Smith, Carson Black, and Shane Finnerty. Thanks to Jamie MacMahan for providing the Echologger EA400 echo sounder used in the *BathyBoard*.

REFERENCES

Bak, A. S., Brodie, K. L., Hesser, T. J., and Smith, J. M. (2019). "Applying dynamically updated nearshore bathymetry estimates to operational nearshore wave modeling." *Coastal Engineering*, 145, 53–64.

Bak, A. S., Durkin, P., Bruder, B., Saenz, M. J., Forte, M. F., and Brodie, K. L. (2023). "Amphibious uncrewed ground vehicle for coastal surfzone survey." *Journal of Surveying Engineering*, 149(4), 04023011.

Birkemeier, W. A. and Mason, C. (1984). "The crab: A unique nearshore surveying vehicle." *Journal of Surveying Engineering*, 110(1), 1–7.

Bourguignon, S., Berger, L., Scalabrin, C., Fablet, R., and Mazauric, V. (2009). "Methodological developments for improved bottom detection with the me70 multibeam echosounder." *ICES Journal of Marine Science*, 66(6), 1015–1022.

Bresnahan, P., Cyronak, T., Brewin, R. J., Andersson, A., Wirth, T., Martz, T., Courtney, T., Hui, N., Kastner, R., Stern, A., McGrain, T., Reinicke, D., Richard, J., Hammond, K., and Waters, S. (2022). "A high-tech, low-cost, internet of things surfboard fin for coastal citizen science, outreach, and education." *Continental Shelf Research*, 242, 104748.

Brewin, R. J. W., de Mora, L., Jackson, T., Brewin, T. G., and Shutler, J. (2015). "On the potential of surfers to monitor environmental indicators in the coastal zone." *PLOS ONE*, 10(7), 1–22.

Brodie, K. L., Bruder, B. L., Slocum, R. K., and Spore, N. J. (2019). "Simultaneous mapping of coastal topography and bathymetry from a lightweight multicamera uas." *IEEE Transactions on Geoscience and Remote Sensing*, 57(9), 6844–6864.

Brodie, K. L., Palmsten, M. L., Hesser, T. J., Dickhudt, P. J., Raubenheimer, B., Ladner, H., and Elgar, S. (2018). "Evaluation of video-based linear depth inversion performance and applications using altimeters and hydrographic surveys in a wide range of environmental conditions." *Coastal Engineering*, 136, 147–160.

Camins, E., de Haan, W. P., Salvo, V.-S., Canals, M., Raffard, A., and Sanchez-Vidal, A. (2020). "Paddle surfing for science on microplastic pollution." *Science of The Total Environment*, 709, 136178.

Dugan, J., Morris, W., Vierra, K., and C.C, P. (2001). "Jetski-based nearshore bathymetric and current survey system." *Journal of Coastal Research*, 17(4), 900–908.

Forte, M. F., Gorrell, L., Elgar, S., Raubenheimer, B., Dickhudt, P. J., and Mitchell, J. R. (2026). "Evaluation of surf zone survey systems during calm and rough sea states." *Journal of Surveying Engineering*, 152(2), 04025021.

Francis, H. and Traykovski, P. (2021). "Development of a highly portable unmanned surface vehicle for surf zone bathymetric surveying." *Journal of Coastal Research*, 37(5), 933–945.

Frugier, S., Almar, R., Bergsma, E. W., and Bak, S. A. (2026). "Standalone color-based bathymetry over 10 years at duck (nc, usa) from optical satellite imagery and wave breaking analysis." *Coastal Engineering*, 203, 104855.

Gallagher, E. L., Boyd, W., Elgar, S., Guza, R., and Woodward, B. (1996). "Performance of a sonar altimeter in the nearshore." *Marine Geology*, 133(3), 241–248.

Gallagher, E. L., Elgar, S., and Guza, R. T. (1998). "Observations of sand bar evolution on a natural beach." *Journal of Geophysical Research: Oceans*, 103(C2), 3203–3215.

Holman, R., Plant, N., and Holland, T. (2013). "cbathy: A robust algorithm for estimating nearshore bathymetry." *Journal of Geophysical Research: Oceans*, 118(5), 2595–2609.

Honegger, D. A., Haller, M. C., and Holman, R. A. (2019). "High-resolution bathymetry estimates via x-band marine radar: 1. beaches." *Coastal Engineering*, 149, 39–48.

Hughes, T. P., Kerry, J. T., Baird, A. H., Connolly, S. R., Dietzel, A., Eakin, C. M., Heron, S. F., Hoey, A. S., Hoogenboom, M. O., Liu, G., McWilliam, M. J., Pears, R. J., Pratchett, M. S., Skirving, W. J., Stella, J. S., and Torda, G. (2018). "Global warming transforms coral reef assemblages." *Nature*, 556(7702), 492–496.

Kimball, P., Bailey, J., Das, S., Geyer, R., Harrison, T., Kunz, C., Manganini, K., Mankoff, K., Samuelson, K., Sayre-McCord, T., Straneo, F., Traykovski, P., and Singh, H. (2014). "The whoi jetyak: An autonomous surface vehicle for oceanographic research in shallow or dangerous waters." *2014 IEEE/OES Autonomous*

Underwater Vehicles (AUV), 1–7.

Lange, A. M., Fiedler, J. W., Merrifield, M. A., and Guza, R. (2023). "Uav video-based estimates of nearshore bathymetry." *Coastal Engineering*, 185, 104375.

Lippmann, T. C. and Smith, G. M. (2009). "Shallow surveying in hazardous waters." *Proceedings of the U.S. Hydrographic Conference*, 454.

Lowe, R. J., Falter, J. L., Bandet, M. D., Pawlak, G., Atkinson, M. J., Monismith, S. G., and Koseff, J. R. (2005). "Spectral wave dissipation over a barrier reef." *Journal of Geophysical Research: Oceans*, 110(C4).

Lowe, R. J., Falter, J. L., Monismith, S. G., and Atkinson, M. J. (2009). "Wave-driven circulation of a coastal reef–lagoon system." *Journal of Physical Oceanography*, 39(4), 873 – 893.

Ludka, B., Guza, R., and O'Reilly, W. (2018). "Nourishment evolution and impacts at four southern california beaches: A sand volume analysis." *Coastal Engineering*, 136, 96–105.

Ludka, B. C., Guza, R. T., O'Reilly, W. C., Merrifield, M. A., Flick, R. E., Bak, A. S., Hesser, T., Bucciarelli, R., Olfe, C., Woodward, B., Boyd, W., Smith, K., Okihiro, M., Grenzeback, R., Parry, L., and Boyd, G. (2019). "Sixteen years of bathymetry and waves at San Diego beaches." *Scientific Data*, 6(1), 161.

Ludka, B. C., Guza, R. T., O'Reilly, W. C., and Yates, M. L. (2015). "Field evidence of beach profile evolution toward equilibrium." *Journal of Geophysical Research: Oceans*, 120(11), 7574–7597.

Luijendijk, A. P., Ranasinghe, R., de Schipper, M. A., Huisman, B. A., Swinkels, C. M., Walstra, D. J., and Stive, M. J. (2017). "The initial morphological response of the sand engine: A process-based modelling study." *Coastal Engineering*, 119, 1–14.

MacMahan, J. (2001). "Hydrographic surveying from personal watercraft." *Journal of Surveying Engineering*, 127(1), 12–24.

Marques, O. B., Feddersen, F., MacMahan, J., Acevedo-Ramirez, C. A., and Suanda, S. H. (2025). "Observations of wave energy dissipation by bottom friction on rocky shores." *Journal of Physical Oceanography*, 55(5), 593 – 610.

Mead, S. and Black, K. (2001). "Predicting the breaking intensity of surfing waves." *Journal of Coastal Research*, 51–65.

Moulton, M., Elgar, S., and Raubenheimer, B. (2014). "Improving the time resolution of surfzone bathymetry using in situ altimeters." *Ocean Dynamics*, 64(5), 755–770.

National Oceanic and Atmospheric Administration (2020). *Operational Risk Assessment Form: GAR*

Evaluation Scale. NOAA Small Boat Program.

O'Reilly, W. C., Olfe, C. B., Thomas, J., Seymour, R. J., and Guza, R. T. (2016). "The california coastal wave monitoring and prediction system." *Coastal Engineering*, 116, 118–132.

O'Dea, A., Anderson, D., Holman, R., Painter, C., and Brodie, K. (2025). "Wave kinematics-based bathymetry estimates from satellite optical video." *Coastal Engineering*, 200, 104753.

Seymour, R., Guza, R., O'Reilly, W., and Elgar, S. (2005). "Rapid erosion of a small southern california beach fill." *Coastal Engineering*, 52(2), 151–158.

Turner, I. L., Harley, M. D., Short, A. D., Simmons, J. A., Bracs, M. A., Phillips, M. S., and Splinter, K. D. (2016). "A multi-decade dataset of monthly beach profile surveys and inshore wave forcing at Narrabeen, Australia." *Scientific Data*, 3(1), 160024.

Welch, P. (1967). "The use of fast fourier transform for the estimation of power spectra: A method based on time averaging over short, modified periodograms." *IEEE Transactions on Audio and Electroacoustics*, 15(2), 70–73.

Work, P. A., Hansen, M., and Rogers, W. E. (1998). "Bathymetric surveying with GPS and heave, pitch, and roll compensation." *Journal of Surveying Engineering*, 124(2), 73–89.

Yates, M. L., Guza, R. T., and O'Reilly, W. C. (2009). "Equilibrium shoreline response: Observations and modeling." *Journal of Geophysical Research: Oceans*, 114(C9).

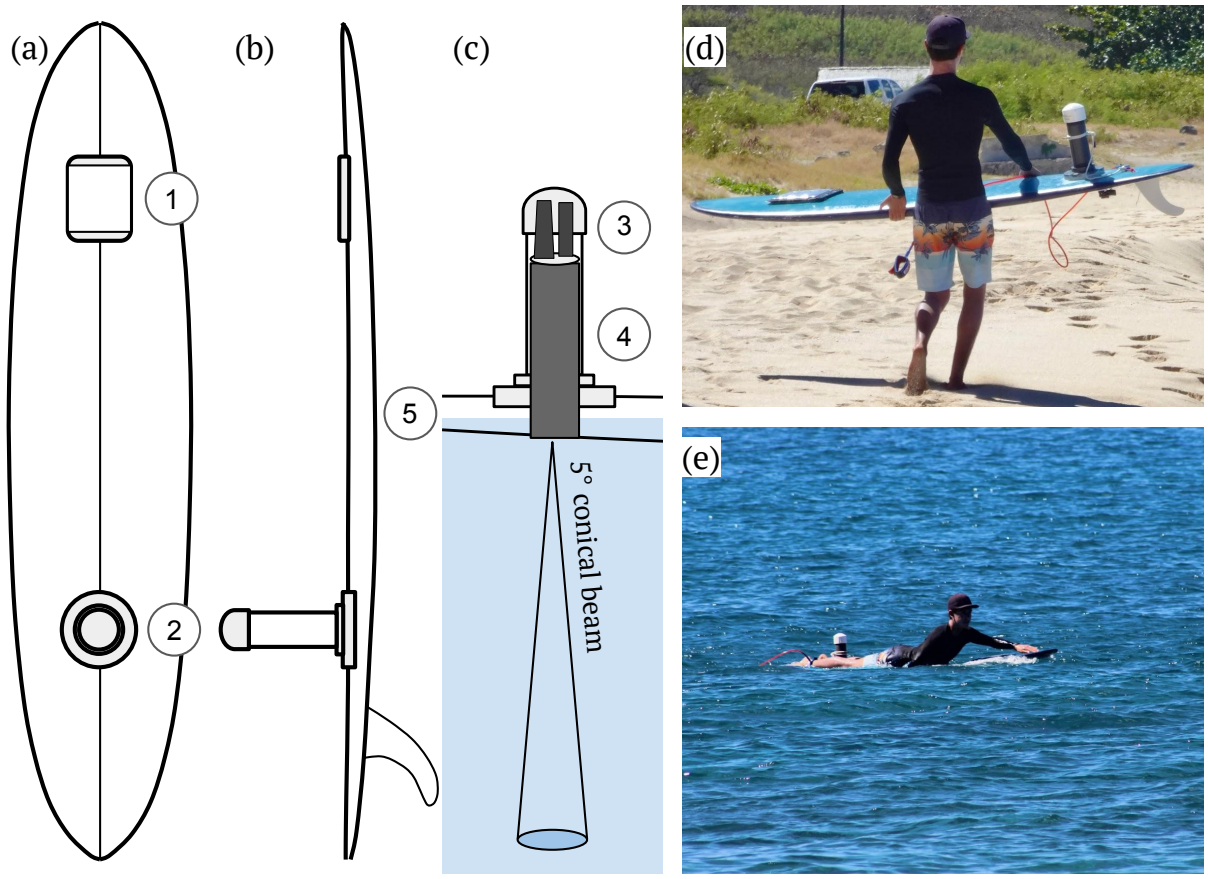


Fig. 1. Simplified drawing of the top (a) and side (b) view of the *BathyBoard*. The navigation tablet (1) is mounted near the nose of the board and the instrument tower (2) is mounted near the tail. (c) Cross-sectional cutaway drawing of the instrument tower, showing the GNSS module (3), echo sounder (4), surfboard (5), approximate water surface elevation, and acoustic beam geometry. The photos in (d)-(e) were taken by Falk Feddersen and show the *BathyBoard* being carried and paddled in the field.

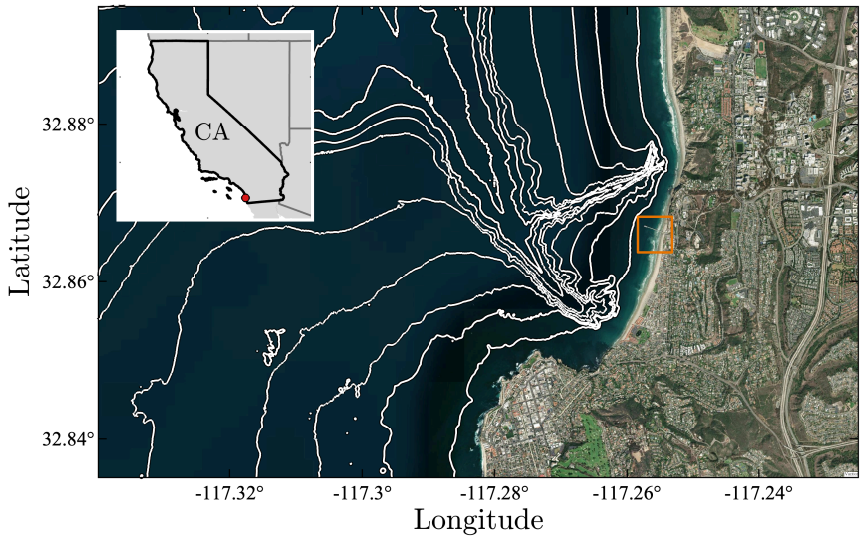


Fig. 2. Overview map of La Jolla, California. White contours show the nearshore bathymetry of La Jolla and Scripps Canyons from NOAA's San Diego Coastal Digital Elevation Model (DEM). The orange box delineates the Scripps Institution of Oceanography survey area used for the Sea-Swell Wave Signal Removal, Jet Ski Based Sonar Comparison, and Repeat-Pass Vertical Uncertainty analyses. The inset shows the location of La Jolla (red point) within California. Basemap: Esri World Imagery; imagery credit: Vantor.

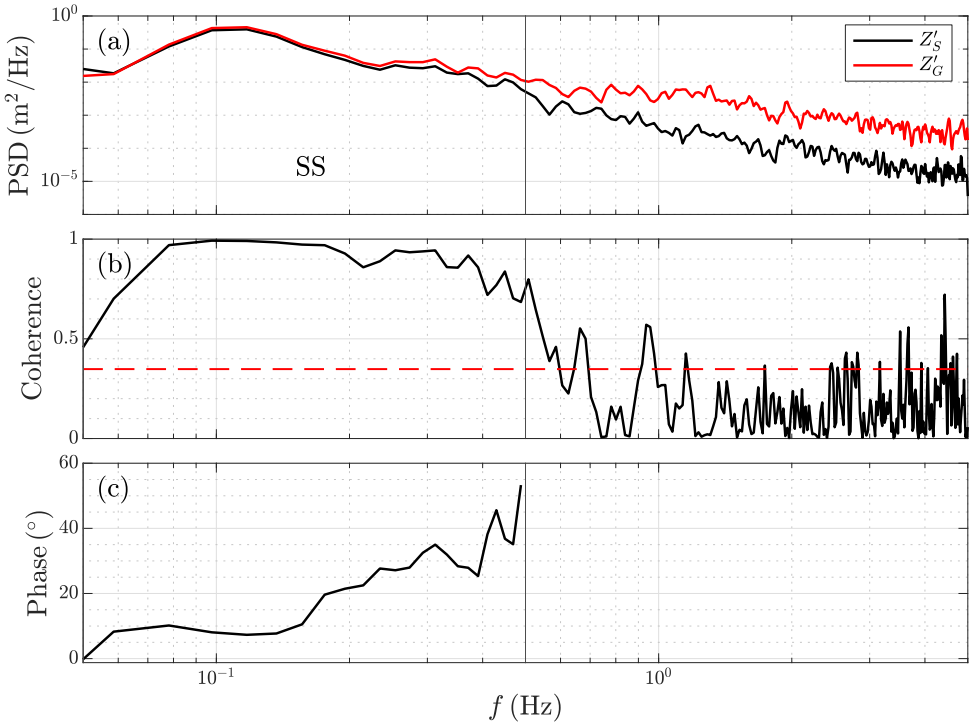


Fig. 3. (a) Power spectral density (PSD) of the echo sounder depth fluctuations, Z'_S, and GNSS elevation fluctuations, Z'_G, as a function of frequency (f) in log–log space. (b) Magnitude-squared coherence between the two signals. The horizontal red dashed line denotes the 95% confidence level. (c) Phase between Z'_S and Z'_G within the sea-swell (SS) frequency band ($0.05 < f < 0.5$ Hz), expressed in degrees.

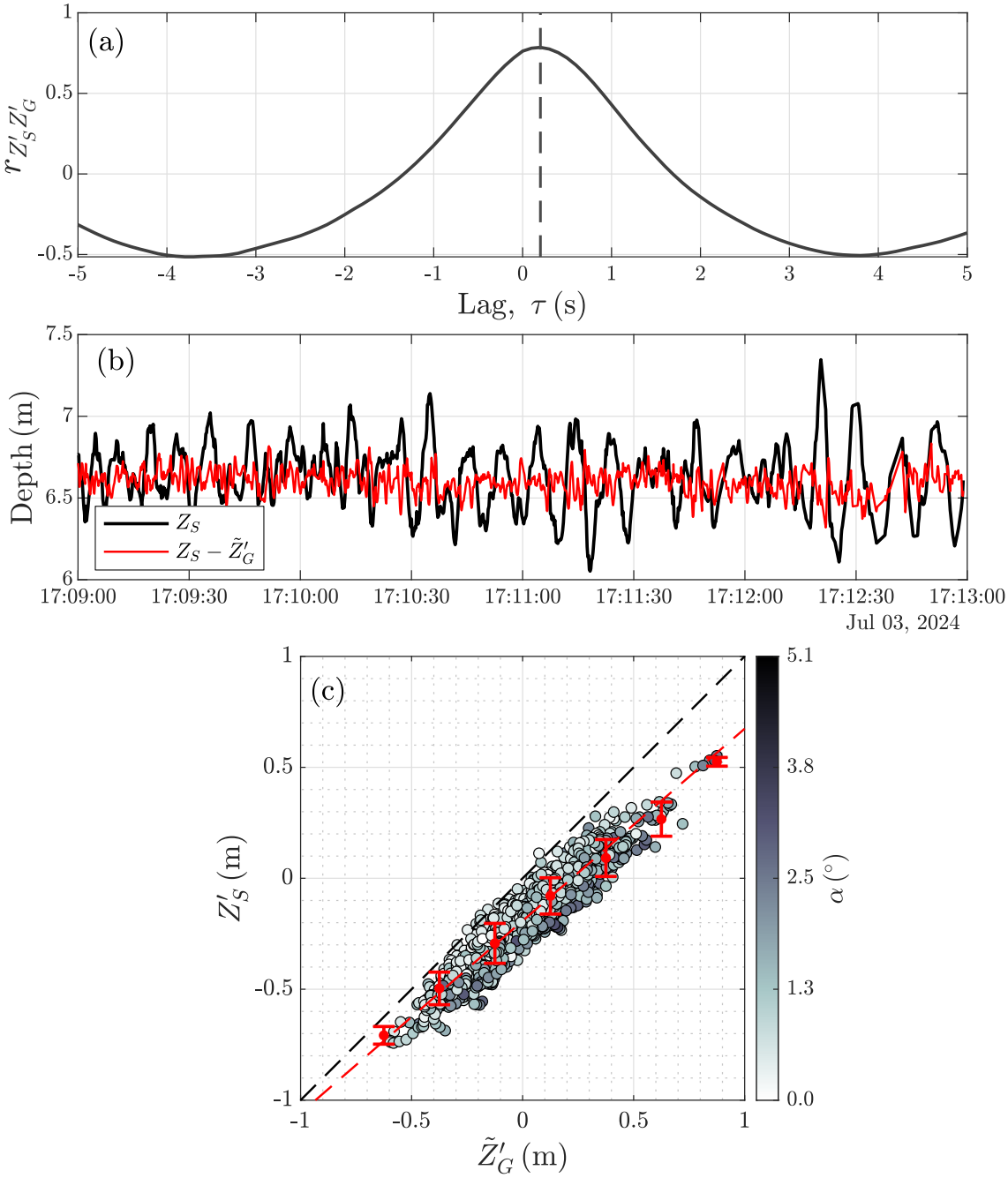


Fig. 4. (a) Cross-correlation between Z_S' and Z_G', where the vertical dashed line represents the time lag τ (0.2 s) at which the correlation is the highest. (b) Time series of echo sounder depth Z_S before (black) and after wave corrections $Z_S - \tilde{Z}_G'$ (red). (c) Comparison of low-pass filtered (cutoff frequency 0.5 Hz) elevation fluctuations from the GNSS receiver ($\tilde{Z}_G'$) and echo sounder depth fluctuations (Z_S') colored by the sensor tilt angle α (2). Binned means and error bars are spaced every 0.25 m. The red dashed line indicates the linear least-squares fit. The black dashed line represents the one-to-one line.

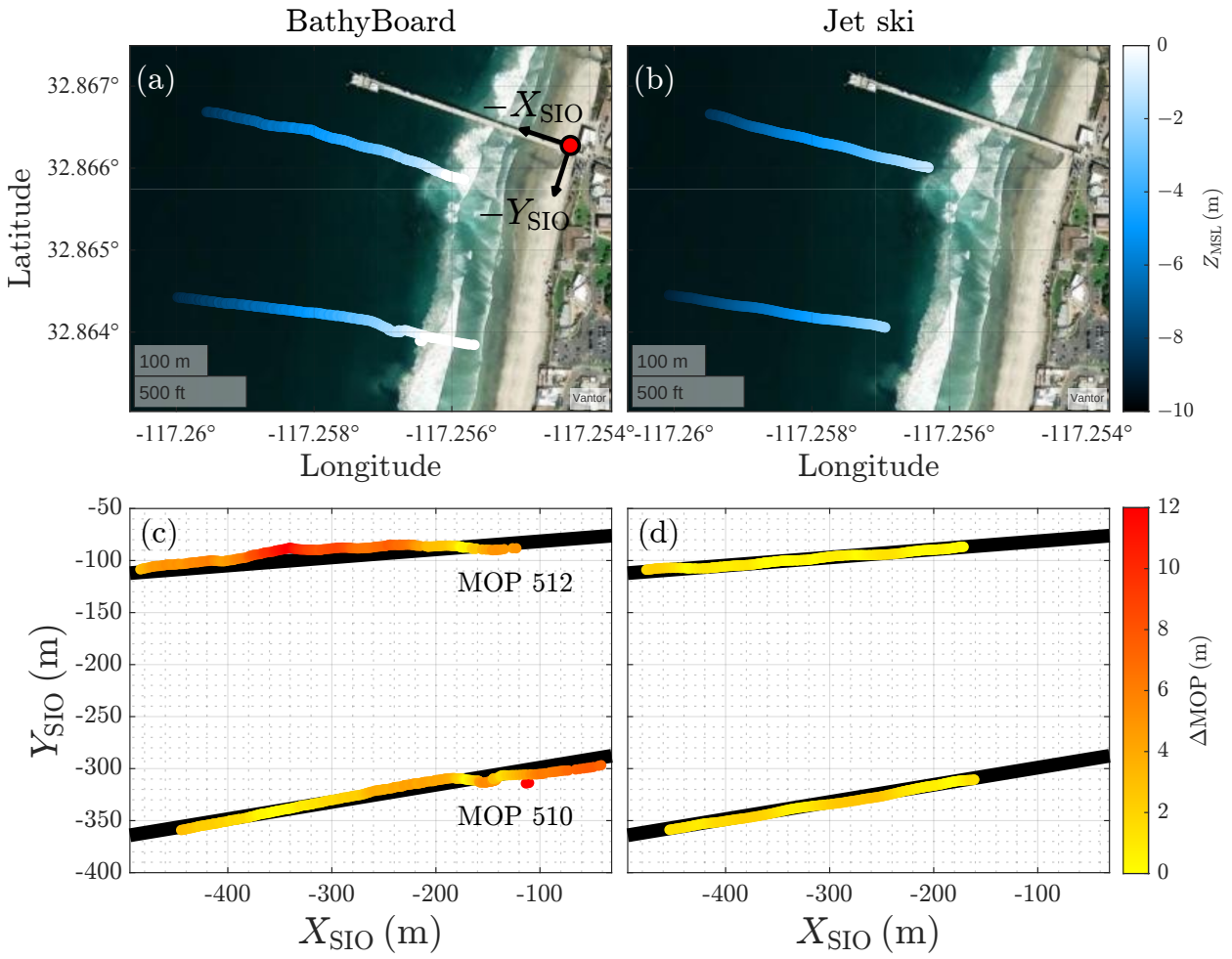


Fig. 5. (a) Two *BathyBoard* survey profiles overlaid on satellite imagery, with points colored by elevation relative to mean sea level Z_{MSL} as a function of latitude and longitude. The red circle represents the origin and black arrows show the direction of the SIO coordinate system in the bottom two panels. (b) Jet ski survey profiles overlaid on the same imagery for comparison. (c) *BathyBoard* shore normal survey profiles from Monitoring and Protection (MOP) lines 512 and 510 transformed to the local SIO coordinate system (see (a)). Points are colored by their perpendicular absolute distance to the corresponding MOP line ΔMOP (m). (d) Jet ski bathymetry profiles from MOP lines 512 and 510 in SIO coordinates colored by ΔMOP (m). Basemap in panels (a) and (b): Esri World Imagery; imagery credit: Vantor.

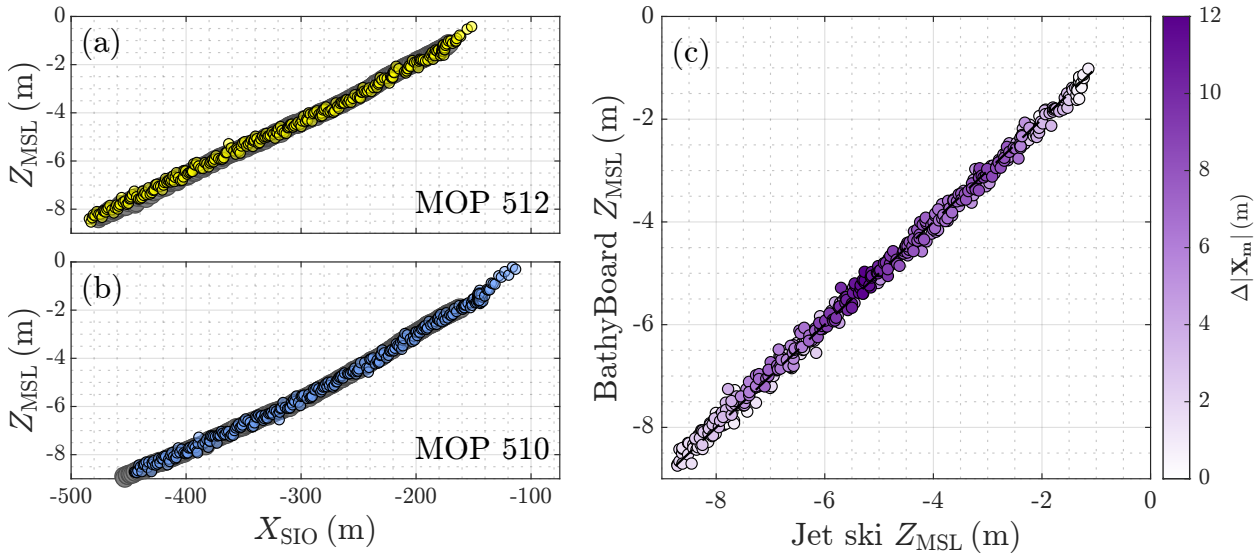


Fig. 6. Cross-shore bathymetric profiles for MOP lines (a) 512 and (b) 510. Gray circles denote jet ski derived bathymetry and *BathyBoard* observations are shown as yellow and blue points. (c) Comparison of elevations using nearest-neighbor matched pairs from both MOP lines, colored by the absolute horizontal distance between matched points. The black dashed line represents a 1:1 slope.

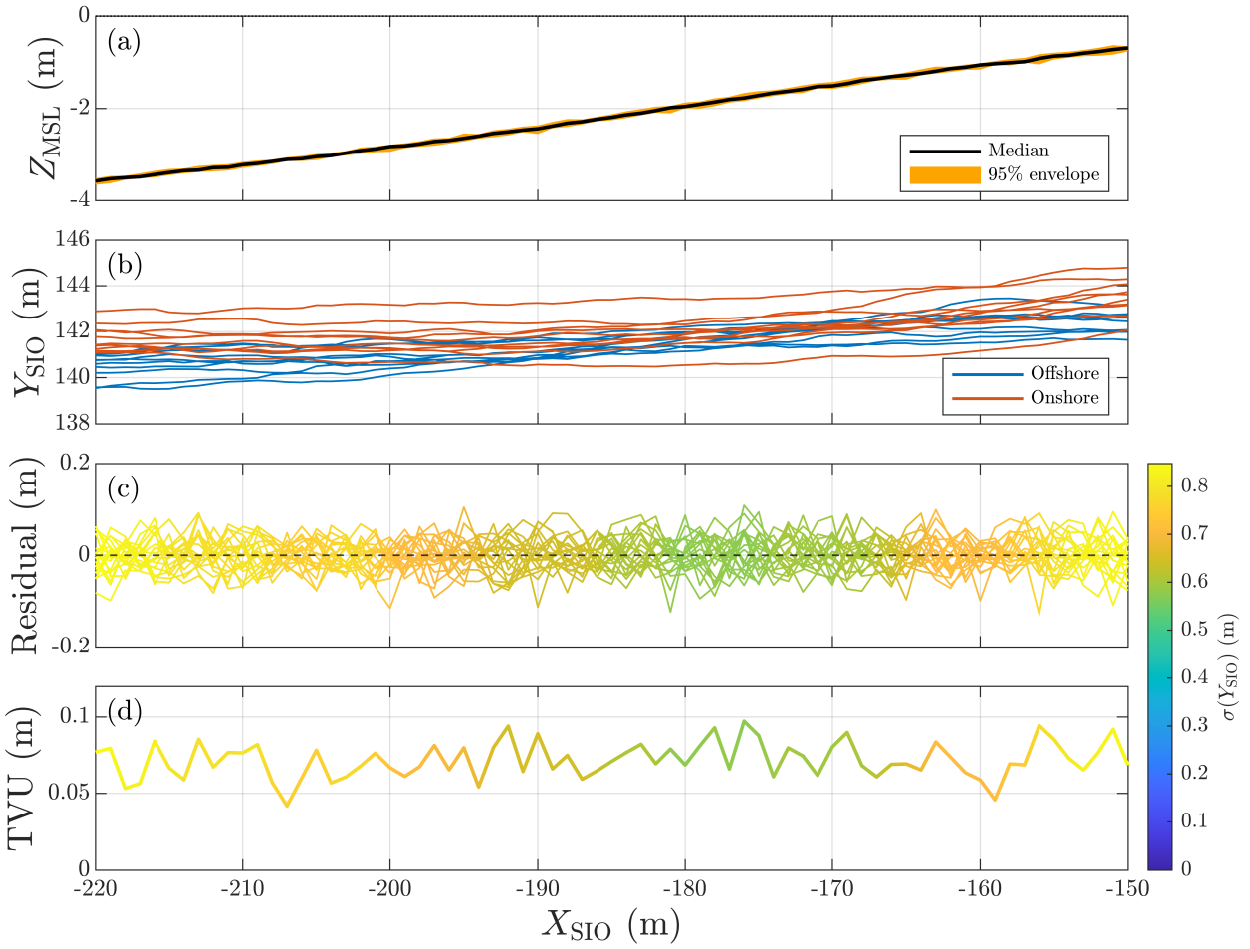


Fig. 7. Repeatability of *BathyBoard* measurements from 20 cross-shore passes (10 out and 10 back). (a) Median bed-elevation profile and 95% envelope of the repeated measurements. (b) Alongshore positions of the offshore-directed (blue) and onshore-directed (red) passes. (c) Elevation residuals relative to the median profile. The horizontal dashed line highlights the median residual. (d) Total vertical uncertainty (TVU) as a function of cross-shore position. Line color in (c) and (d) indicates the standard deviation of the alongshore sampling position, $\sigma(Y_{\mathrm{SIO}})$.

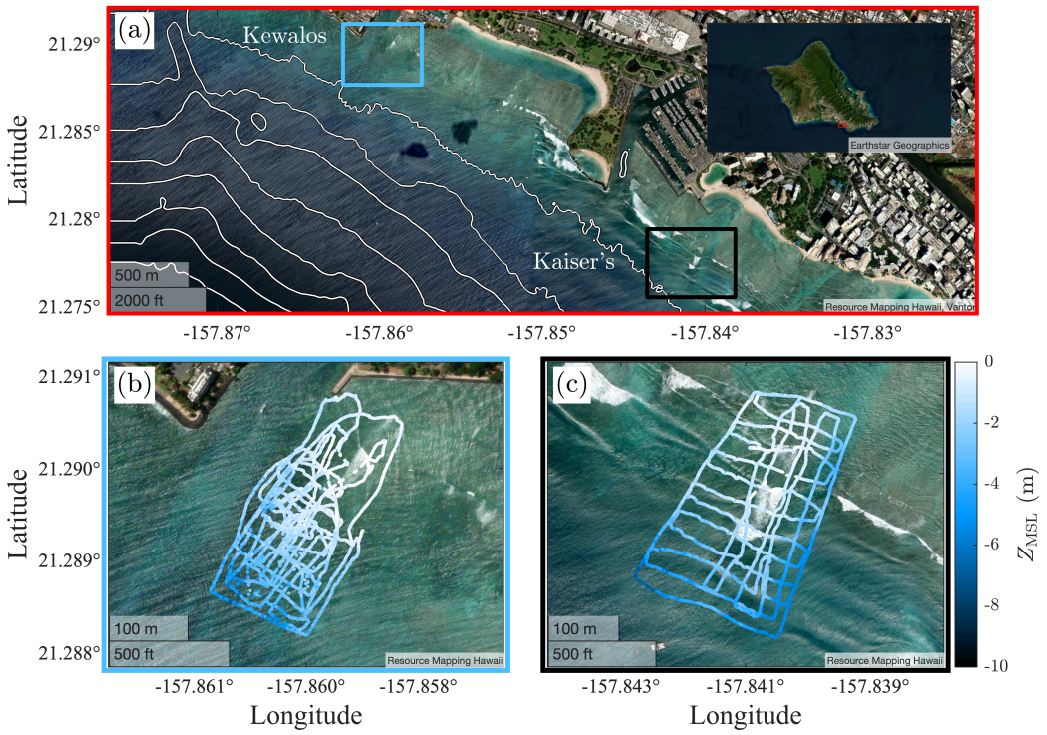


Fig. 8. (a) Satellite imagery showing the location of the Ala Moana/Waikiki coastal area on the south shore of O'ahu (inset). Nearshore bathymetry is denoted by white contours from NOAA's Honolulu Coastal DEM. *BathyBoard* paddle tracks overlaid on satellite imagery in latitude/longitude coordinates at (b) Kewalos and (c) Kaiser's. Tracks are colored by depth referenced to mean sea level (Z_{MSL}). Basemap: Esri World Imagery. Imagery credits: (a) Resource Mapping Hawaii and Vantor; inset: Earthstar Geographics; (b, c) Resource Mapping Hawaii.

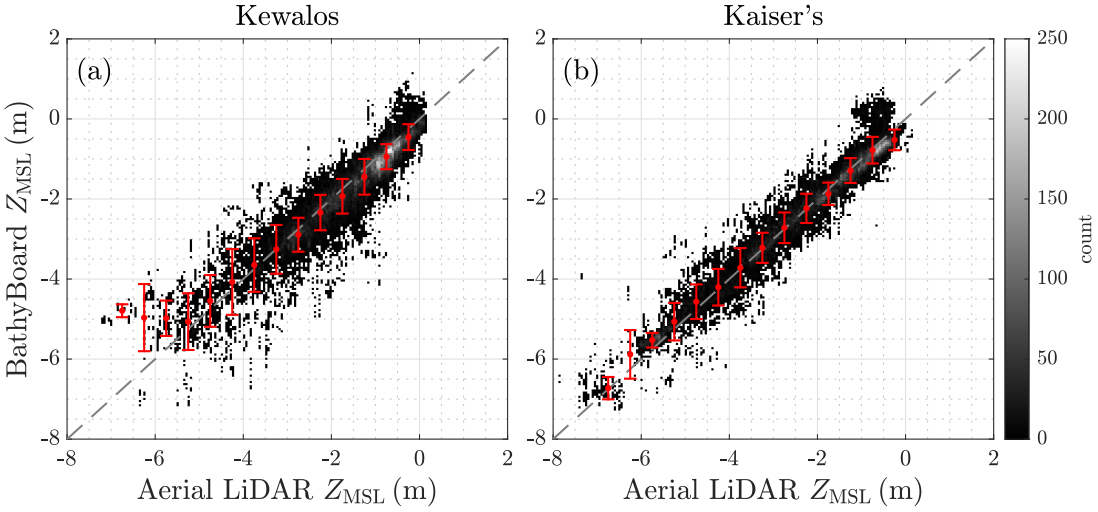


Fig. 9. 2-D histogram comparison between the Aerial LiDAR depth and *BathyBoard* depth at (a) Kewalos and (b) Kaiser's, colored by count within bins. Binned means and error bars are spaced every 0.5 m. The gray dashed lines represent the 1:1 slope.